Specific Interactions and Ionic Aggregation in Miscible Blends of Nylon-6 and Zinc Sulfonated Polystyrene Ionomer

Xinya Lu and R. A. Weiss*

Polymer Science Program and Department of Chemical Engineering, University of Connecticut, Storrs, Connecticut 06269-3136

Received March 9, 1992; Revised Manuscript Received July 20, 1992

ABSTRACT: Blends of a lightly sulfonated polystyrene (10.1 mol % sulfonation) neutralized with zinc (ZnSPS) and nylon-6 (N6) were found to be miscible over the entire compositional range. Miscibility was a consequence of transition metal complexation between the metal sulfonate and the amide groups. Melting point depression data gave a value for the polymer–polymer interaction parameter of $\chi = -1.3$, which indicates very strong intermolecular interactions. FTIR and SAXS analyses indicated that the polyamide effectively solvated the ionic associations in the blends.

Introduction

The use of ionomers to introduce specific interactions between components in a polymer blend can result in miscible or partially miscible blends of two otherwise immiscible polymers.[1,2] Such interactions include hydrogen bonding,[3] ion–dipole interactions,[4] acid–base interactions,[5] or transition metal complexation.[6] Often, the extent of interaction can be controlled by the choice of the acid group and/or the counterion, which provides considerable control of the extent of mixing and the morphology and final properties of the blend.

Blends containing ionomers have been used to improve the impact strength and moisture barrier properties of polyamides. For example, poly(ethylene-*co*-methacrylic acid) (PEMA) and nylon-6 blends have been studied by a number of laboratories.[7-10] Matzner et al.[11] reported that blends of poly(ethylene-*co*-acrylic acid) and N6 were miscible, as evidenced by a single, broad T_g, and Kuphal et al.[12] found that poly(styrene-*co*-acrylic acid) was miscible with N6 when the copolymer contained 20 wt % acrylic acid. The phase behavior of lightly sulfonated polystyrene ionomers (SPS) and polyamides as a function of sulfonation level and the counterion has been investigated in our laboratory.[13-15] Hydrogen bonding and complex formation between the cation and the amide group were responsible for miscibility of various SPS ionomers and N6, as evidenced by a single composition-dependent T_g and negative values of the Flory–Huggins interaction parameter, χ, measured from melting point depression data. For a fixed sulfonation level, χ depended on cation in the order Mn < Zn < Li < H; i.e., the transition metal salts of SPS exhibited the most effective miscibility enhancement. Recently, Molnar and Eisenberg have also examined miscibility of N6 with the acid form or alkali salt (Li and Na salts) of SPS as a function of sulfonation level.[16]

One important feature of an ionomer is the strong molecular associations that occur between ionic groups that lead to phase-separated ion-rich domains, often called clusters. In a miscible blend involving an ionomer and a nonionic polymer, the development of the cluster morphology will undoubtedly be affected by the specific interactions of the ionic groups with the other polymer as well as the composition of the blend. Microstructural characterization of ionic aggregates in miscible ionomer blends may provide useful information that should help shed light on some unanswered questions about cluster morphology in neat ionomers.

This paper describes a study of miscible blends of N6 and the zinc salt of lightly sulfonated polystyrene ionomers (ZnSPS). Differential scanning calorimetry (DSC) was used to determine miscibility and χ. Fourier transform infrared spectroscopy (FTIR) was used to characterize the local environment of the Zn sulfonate groups as a function of the blend composition. This yielded information about the specific interactions between ZnSPS and N6 as well as about the ionic associations within ZnSPS. Small-angle X-ray scattering (SAXS) was employed to investigate the microstructural changes in the blends, specifically the effect on the cluster morphology.

Experimental Section

Materials. Lightly sulfonated polystyrene (SPS) was prepared according to the procedure described by Makowski et al.[17] The number-average and weight-average molecular weights of the starting polystyrene were 106 000 and 288 000, respectively, as determined by gel permeation chromatography (GPC). The sulfonation level was 10.1 mol %, as determined by titration of SPS in toluene/methanol (90/10 v/v) solution to a phenolphthalein end point using sodium hydroxide in methanol. The zinc salt (ZnSPS) was prepared by neutralizing the SPS in toluene/methanol with a 20% excess of zinc acetate dihydrate in methanol. The ZnSPS was precipitated in a large excess of ethanol, filtered, washed several times with ethanol, and dried at 70 °C for 1 week under vacuum. N6 with a weight-average molecular weight of 24 000 was obtained from Polysciences Inc.

Blends of N6 and ZnSPS were prepared by mixing in solution. A solution of N6 in *m*-cresol was added dropwise into a stirred solution of ZnSPS in *m*-cresol/dimethylformamide (60/40 v/v). Films of the blends were cast from solution at 120 °C and dried at 90 °C for 2 weeks under vacuum.

SAXS Measurements. Small-angle X-ray scattering data were collected by using a pinhole collimation camera and a TEC Mode 200 linear position-sensitive detector. Fe Kα radiation (λ = 0.19373 nm), monochromatized with a manganese filter was obtained from a rotating-anode source operating at 40 kV and 200 mA. A sample-to-detector distance of 52 cm and a pinhole diameter of 0.15 mm were used, and the detector had a usable length of ca. 10 cm. These conditions yielded a q range of 0.25–6.0 nm^{-1}, where $q = 4\pi \sin\theta/\lambda$, λ is the X-ray wavelength, and 2θ is the scattering angle. The detector had 256 channels, corresponding to a resolution of $\approx$0.03 nm^{-1}. All the data were corrected for the detector sensitivity, parasitic and background scattering, and sample absorption. The background correction factor was determined by a fitting the high-q region according to the procedure of Porod.[18]

DSC Measurements. Differential scanning calorimetry thermograms were obtained with a Perkin-Elmer DSC-7 using a heating rate of 20 °C/min. The glass transition temperature, T_g, was defined as the midpoint of the change in heat capacity at the transition. The melting point, T_m, was taken as the maximum of the melting endotherm. A cold-crystallization temperature was characterized by holding the sample at 240 °C,

0024-9297/92/2225-6185$03.00/0

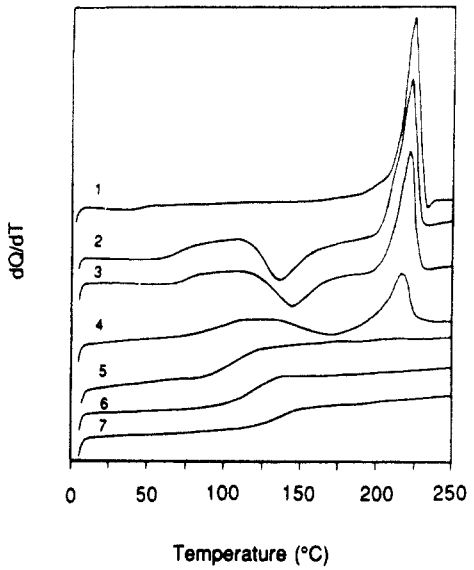

Figure 1. DSC thermograms of N6/ZnSPS blends quenched from 240 °C; wt % ZnSPS: (1) 0%, (2) 10%, (3) 20%, (4) 60%, (5) 70%, (6) 90%, (7) 100%.

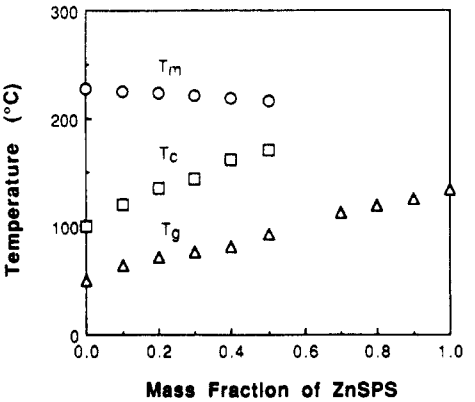

Figure 2. Thermal transitions versus composition for N6/ZnSPS blends quenched from 240 °C; T_g = glass transition temperature of the blend, T_c = cold crystallization temperature of N6, T_m = melting point of N6.

which was above T_m, for 5 min, quickly quenching the specimen to 0 °C, and reheating to 250 °C at 20 °C/min. The crystallization temperature, T_c, was defined as the maximum of the crystallization exotherm observed above T_g during the reheating scan. The equilibrium melting point was determined according to the method of Hoffman and Weeks.[19]

FTIR Measurements. Infrared spectra were obtained on a Nicolet Model 60SX Fourier transform infrared spectrometer. A total of 128 scans at a resolution of 1 cm^{-1} were signal averaged. The samples were cast on NaCl plates from solution and dried under vacuum at 120 °C for 2 weeks.

Results and Discussion

Thermal Analysis. DSC thermograms of the component polymers and the blends are shown in Figure 1. The samples were quenched from 240 °C prior to the DSC scan and, as such, represent the phase behavior at 240 °C. The blends exhibited a single composition-dependent T_g intermediate between those of the neat components (Figure 2). Based on the criterion of a single T_g, the ZnSPS and N6 were judged to be miscible over the entire range of composition at 240 °C.

Further evidence for the miscibility of the two polymers was the increase in the cold crystallization temperature of the N6 crystallites, T_c, and the depression of the melting temperature, T_m, as the ZnSPS content increased (Figure 2). No crystallinity was observed when the ZnSPS concentration exceeded 60%. The increase of T_c was a direct consequence of the increase of T_g as the blend composition became more ZnSPS-rich. The melting point depression of the N6 was the result of the strong specific interactions that occurred between N6 and ZnSPS; the nature of these interactions will be discussed later in this paper. Equilibrium melting points were measured from Hoffman–Weeks plots,[19] and the Flory–Huggins segmental interaction parameter, χ, was calculated for the blend using the Nishi–Wang equation[20]

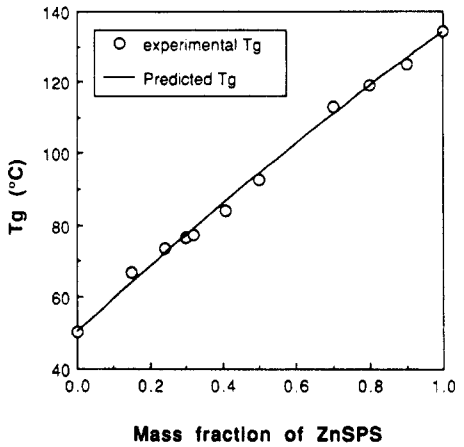

Figure 3. Comparison between experimental and predicted (eq 2 in text) T_g's versus composition for N6/ZnSPS blends quenched from 240 °C.

$$\frac{1}{T_m} - \frac{1}{T_m^\circ} = -\frac{\chi R V_{u2}}{\Delta H_{u2} V_{u1}} \phi_1^2 \qquad (1)$$

where T_m and T_m° are the equilibrium melting points of the crystallizable component in the blend and in the neat N6, respectively. Subscripts 1 and 2 refer to the noncrystallizable blend component, ZnSPS, and the crystallizable polymer, N6, respectively. ϕ_i, V_{ui}, and ΔH_{ui}, are the volume fraction, molar volume, and molar enthalpy of fusion of component i. ΔH_{u2} was taken as 18.1 kJ/mol,[21] and V_{u2} was calculated from the density of amorphous N6. The calculated value of χ was −1.3, which indicates very strong interactions between the two polymers.

In Figure 3, the T_g data for the blends are plotted as a function of the composition in the amorphous phase that was obtained by correcting for the crystallinity in the sample. The solid curve represents the predictions of the Lu–Weiss theory,[22] eq 2, using $\chi = -1.3$.

$$T_g = \frac{w_1 T_{g1} + k w_2 T_{g2}}{w_1 + k w_2} - \frac{A w_1 w_2}{(w_1 + k w_2)(w_1 + b w_2)(w_1 + c w_2)^2}$$

$$A = \frac{\chi R (T_{g2} - T_{g1}) c}{M_1 \Delta C_{p1}} \qquad (2)$$

where w_i, T_{gi}, and ΔC_{pi} are, respectively, the weight fraction, glass transition temperature, and the heat capacity change at T_{gi} for component i. $k = \Delta C_{p2}/\Delta C_{p1}$, and b is the ratio of the amorphous densities of polymer 2 and polymer 1. Good agreement was found between the experimental values and those predicted from the theory represented by eq 2.

FTIR Spectroscopy. In a previous paper[14] it was shown by FTIR spectroscopy that hydrogen bonding of the sulfonate and amide groups and complexation between the transition metal cation and the amide nitrogen occurred in blends of MnSPS and N6. This conclusion was based on three observations that were fully discussed in ref 14:

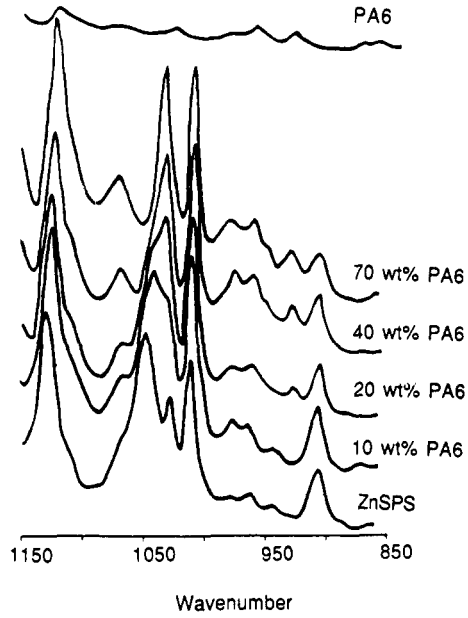

Figure 4. FTIR spectra of N6/ZnSPS blends in the region 850–1150 cm^{-1}.

(1) shifts of the in-plane skeleton vibration of the sulfonated benzene at ca. 1130 cm^{-1} and the symmetric stretching of the sulfonate anion vibration at ca. 1046 cm^{-1}, (2) broadening of the hydrogen-bonded N–H stretching band centered around 3300 cm^{-1} and the resolution of an absorption for non-hydrogen-bonded N–H stretching at 3410 cm^{-1} (the latter band was shifted to lower frequency from what is expected for non-hydrogen-bonded N–H stretching as a result of complexation with the Mn(II) cation), and (3) development of a new absorption at ca. 3520 cm^{-1} that was attributed to delocalization of the lone pair of electrons on the amide nitrogen by the Mn(II) cation.

The current study concentrated on the changes in the local environment of the Zn sulfonate groups as the composition of ZnSPS/N6 blends was changed. Figure 4 shows the infrared spectra of the neat ZnSPS and the blends in the region from 850 to 1150 cm^{-1}, which is associated with the stretching vibration region of the sulfonate group. Band assignments in this region were based on the infrared spectrum of fully sulfonated polystyrene that is fully described in a monograph by Zundel.[23] The broad band at 1045 cm^{-1} was due to the symmetric stretching vibrations of the S–O bond of $SO_3^-(Zn^{2+})_{1/2}$. The asymmetric stretching vibration of the sulfonate anion was a doublet centered around ca. 1200 cm^{-1}, but in this case, the higher frequency absorption was unresolved due to other bands arising from the polystyrene in this region. The absorptions at 1135 and 1070 cm^{-1} in the neat ZnSPS resulted from the in-plane skeleton vibrations of the benzene ring and that substituted by a sulfonate anion, respectively. The absorption at 1029 cm^{-1} was the in-plane bending vibration of the benzene ring, and the band at 1011 cm^{-1} was also due to the in-plane bending vibrations of the benzene ring but coupled by the symmetric S–O stretching vibration of the sulfonate anion.

For fully sulfonated polystyrene, Zundel[23] found that the symmetric stretching vibration of the sulfonate anion was particularly sensitive to the local environment of the sulfonate group. A stronger local electrostatic field shifts this band to higher frequency. For example, this vibration occurs at ca. 1037 cm^{-1} for the Zn salt of fully sulfonated polystyrene and at ca. 1033 cm^{-1} for the fully hydrated

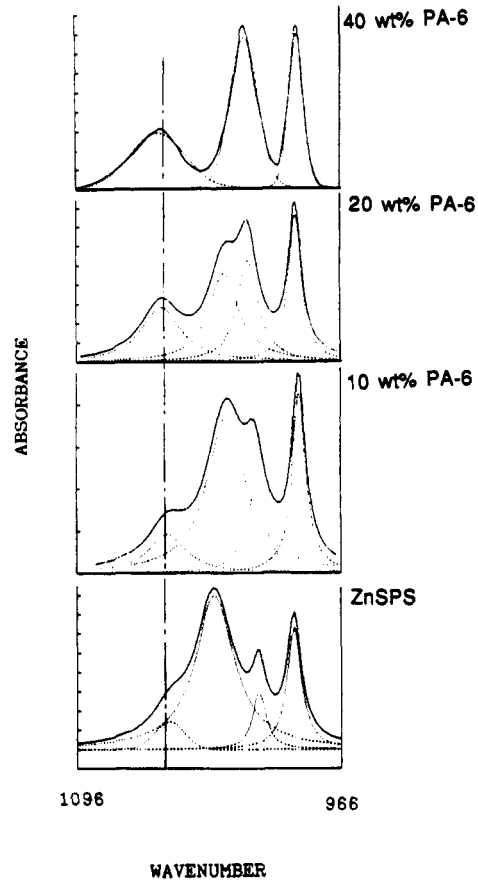

Figure 5. Deconvolution of the sulfonate anion stretching region of the FTIR spectra of N6/ZnSPS blends.

sulfonic acid. For the neat ionomer, however, the symmetric stretching vibration shifted to higher frequency, i.e., to 1045 cm^{-1}.

The major morphological difference between the ZnSPS ionomer and fully sulfonated polystyrene is expected to be the microphase separation exhibited by the ionomer. This may lead to two different local environments of the SO_3^- anion: that of associated sulfonate groups in ionic clusters or multiplets and that of unassociated ones in a nonionic matrix. As a result, one might expect to observe two separate symmetric stretching bands due to the associated SO_3^- and unassociated SO_3^-. The band due to associated SO_3^- should be at higher wavenumber. In the dry neat ionomer, most of ionic groups are associated, and the symmetric stretching band of the anion was observed at ca. 1045 cm^{-1}. This band shifts to ca. 1034 cm^{-1} when the ionic association is disrupted by a polar solvent.[22] It seems reasonable to assign the bands at 1045 and 1034 cm^{-1} to associated and unassociated, or solvated, sulfonate groups, respectively.

The spectra of the blends in Figure 4 show a decrease of the intensity of the band at 1045 cm^{-1} and a concurrent increase of the intensity of a band at ca. 1030 cm^{-1} with increasing N6 addition. The band at ca. 1030 cm^{-1} is believed to be a composite absorption composed of the symmetric stretching vibration of the "solvated" anion at ca. 1034 cm^{-1} and the in-plane bending vibration of the benzene ring of polystyrene at ca. 1029 cm^{-1}. The latter absorption is not expected to be influenced by the N6 addition. The region of the FTIR spectra between 1096 and 966 cm^{-1} is shown in Figure 5, in which the spectra were resolved into four components using Gaussian band shapes. Upon addition of 10% (by weight) N6 to ZnSPS, the 1045-cm^{-1} band shifted to 1039 cm^{-1} and the ratio of intensities I_{1039}/I_{1030} decreased. This is consistent with

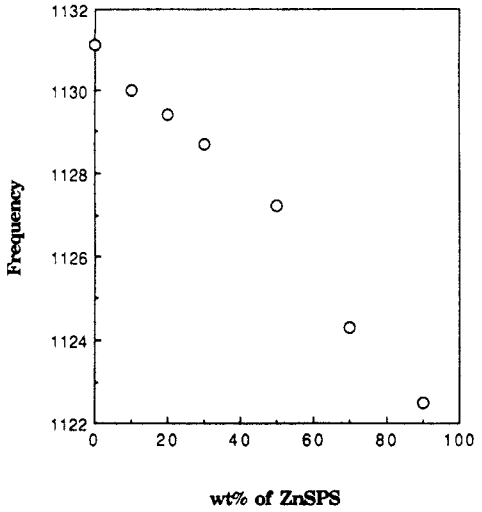

Figure 6. Frequency of the asymmetric stretching vibration of the zinc sulfonate group as a function of blend composition.

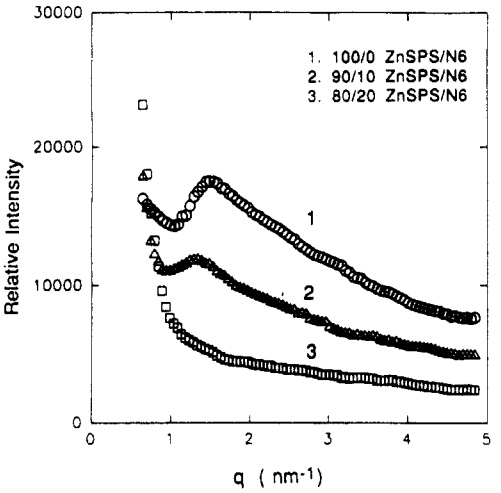

Figure 7. SAXS intensity versus scattering vector for ZnSPS and N6/ZnSPS blends.

the explanation given above that association of the N6 with either the anion or the cation effectively weakens the force constant of the ion pair. The change in the intensity ratio of the two bands indicates that the population of the solvated sulfonate groups increased, presumably as a direct consequences of the intermolecular interactions of the amide and sulfonate groups. It is not unexpected that the presence of a small amount of the polar N6 weakens the ion pair. Mixing N6 with ZnSPS on a segmental level increases the effective dielectric constant of the medium surrounding the sulfonate group, which weakens the electrostatic force, F, between the ion pair

$$F = q^+q^-/\epsilon r^2 \tag{3}$$

where q^+ and q^- are the charges on the ions, ϵ is the dielectric constant of the medium, and r is the separation of the ions.[23]

When the N6 concentration was increased from 10% to 20%, the 1030-cm^{-1} band shifted to 1034 cm^{-1} and I_{1039}/I_{1034} decreased further; 1034 cm^{-1} is the position of the anion symmetric stretching vibration reported by Fitzgerald and Weiss[24] for ZnSPS/dimethylformamide mixtures, in which the anion is fully solvated. The increase in the lower frequency band at 1034 cm^{-1} is probably a consequence of the increased concentration of solvated anion and the dominance of the 1034-cm^{-1} absorption over the 1029-cm^{-1} polystyrene absorption. When the concentration of N6 reached 40%, the higher frequency 1045-cm^{-1} band disappeared and a single band at ca. 1034 cm^{-1} was observed.

The in-plane stretching vibration of benzenesulfonate at 1130 cm^{-1} also shifted to lower frequency when N6 was blended with ZnSPS (see Figure 4). Figure 6 shows the frequency of this band as a function of the blend composition. The progressive shift to lower frequency with increasing N6 is indicative of a weakening of the cation's influence on the anion, similar to what is observed when the sulfonated group is hydrated. Two explanations may account for this: (1) hydrogen bonding between the amide group and the anion oxygen and/or (2) complexation of the Zn cation with the lone pair of electrons on the amide nitrogen.

SAXS Analysis. Microphase separation of ion-rich domains in ionomers is characterized by a peak commonly observed by small-angle X-ray scattering (SAXS). Figure 7 compares the SAXS curves for ZnSPS and two ZnSPS/N6 blends containing 10%, and 20% (by weight) N6. Since all the samples were amorphous, as determined by DSC, there was no interference in the SAXS curves due to the long spacing of crystalline lamellae. The peak at ca. q = 1.5 nm^{-1} (corresponding to a characteristic distance of ca. 4.2 nm) in the neat ZnSPS is due to aggregates rich in Zn sulfonate groups. With the addition of 10% N6, the ionic peak shifted to q = 1.3 nm^{-1}, corresponding to a characteristic size of 4.8 nm, and the intensity became noticeably weaker. The peak was not detected for the blend containing 20% N6, which indicates that the ionic microstructure was absent. In both blends, the ZnSPS and the N6 were miscible in the amorphous phase, at least on the scale probed by DSC, though in the 10% N6 blend, some microphase separation of the ionomer persisted. The disappearance of the SAXS peak, i.e., microphase separation, was due to solvation of the ionic species by the N6.

The SAXS peak intensity is determined by two factors: (1) the volume fraction of the ionic aggregates in the sample and (2) the electron density contrast between the microphase-separated ionic aggregate and the ion-poor continuous phase. N6 and polystyrene have nearly equivalent electron densities, 0.60 and 0.61 mol/cm^3, respectively, so the addition of a small amount of N6 should have an insignificant effect on the electron density contrast if the N6 partitioned into the nonionic phase. Similarly, the decrease in intensity cannot be fully accounted for by the dilution of the ZnSPS with N6. This indicates that the intensity decrease must be due to a decrease in the electron density of the aggregates by swelling with N6 and/or a decrease in the volume fraction of aggregates. Both explanations are consistent with the FTIR results that indicated that N6 interacts strongly with the metal sulfonate groups; in this case, it essentially acts as a solvent for the ionic associations. The disappearance of the ionic peak for the 20% N6 sample indicates that either microphase separation did not occur in this sample or the peak has shifted to a value of q too low to be resolved by the SAXS geometry employed in these experiments; i.e., the characteristic spacing due to aggregates was greater than 6.0 nm (corresponding to $q \sim 1$ nm^{-1}).

The shift of the ionic peak of ZnSPS to lower angle by the addition of N6 is similar to the effect of water on the SAXS curves of perfluorosulfonate[25] and SPS ionomers.[26,27] The origin of the ionic peak in ionomers is an unresolved question, though various models of ionic clusters have been proposed. These models can be divided into two categories, those that attribute the peak to *inter*particle interference and those that attribute it to *intra*particle interference. The intraparticle model would attribute the shift of the ionic peak observed here to

swelling of the clusters, while the interparticle model would indicate that the distances between clusters increase. In either case, the changes result from association of the polyamide with the ionic groups.

If the ionic aggregate is assumed to have a sharp interface, to have a constant electron density, and to represent a small volume fraction of the sample, the asymptotic form of the scattered intensity is[18]

$$\frac{\lim_{q\to\infty} I(q)q^4}{\int_0^\infty I(q)q^2\,dq} = \frac{K_p}{Q} = \frac{S}{\pi V} \tag{4}$$

where K_p and Q are the Porod constant and the scattering invariant, respectively. S/V is the specific interfacial area, from which a particle size can be calculated if the shape were known. Assuming a spherical shape for the ionic aggregates, the radii, R_a, of the aggregates in the ZnSPS ionomer and the 90/10 ZnSPS/N6 blend were estimated to be 0.74 and 0.51 nm, respectively.

Another feature of the SAXS curves of ionomers is a large intensity upturn at small angles, zero-angle scattering, which is considered to arise from an inhomogeneous distribution of ionic aggregates within the sample[28] or from a nonrandom distribution of unaggregated ionic groups.[29] A kinetic study by Galambos et al.[30] of the formation of the ionic peak in MnSPS supported the latter assignment. For the SAXS data in Figure 7, the zero-angle scattering increased with increasing N6 concentration. This result also appears to support the interpretation of the origin of the zero-angel scattering being due to unaggregated ionic groups and the idea that the polyamide solvates the ionic clusters.

Conclusion

A zinc sulfonated polystyrene ionomer and nylon 6 formed miscible blends over the entire range of composition, as determined by a single composition-dependent T_g. The interaction parameter of the blends calculated from melting point depression data has a large negative value, which indicates the presence of strong interactions between the two polymers. FTIR spectroscopy confirmed that specific interpolymer interactions occurred between the zinc sulfonate and amide groups.

The FTIR spectra also suggested that the Zn sulfonate groups in the blends existed in two different environments: aggregated or associated Zn sulfonate groups and isolated sulfonate groups, solvated by polyamide. With increasing N6 concentration, the population of unassociated sulfonate groups increased and that of associated species decreased. At an N6 concentration of 40% (by weight), it appeared that all the sulfonate group associations were solvated.

The solvation effect of N6 on the ionic aggregation of ZnSPS was demonstrated by SAXS measurements. Addition of 10% (by weight) of N6 to ZnSPS lowered the intensity of the ionic peak and shifted it to lower angle. At 20% (by weight) of N6, the ionic peak was not observed. Like the FTIR results, these SAXS data indicated that in the miscible blends of ZnSPS and N6, the aggregated Zn sulfonate groups were effectively dissociated by the amide group. In addition, an increase in the zero-angle scattering with the addition of N6 was consistent with the idea that this SAXS feature was due to isolated ionic groups.

Acknowledgment. We are grateful for the support of this research by the Polymers Program of the National Science Foundation, Division of Materials Research, Grant DMR 88-05981, and the Consortium for Polymer Compatibilization Research at the University of Connecticut.

References and Notes

(1) Natansohn, A.; Murali, R.; Eisenberg, A. *Makromol. Chem., Macromol. Symp.* **1988**, *16*, 175.
(2) Weiss, R. A.; Beretta, C.; Sasongko, S.; Garton, A. *J. Appl. Polym. Sci.* **1990**, *41*, 91.
(3) Ziska, J. J.; Barlow, J. W.; Paul, D. R. *Polymer* **1981**, *22*, 918.
(4) Eisenberg, A.; Hara, M. *Polym. Eng. Sci.* **1984**, *24*, 1306.
(5) Zhow, Z. L.; Eisenberg, A. *J. Polym. Sci., Polym. Phys. Ed.* **1983**, *21*, 223.
(6) Sen, A.; Weiss, R. A.; Garton, A. In *Multiphase Polymers: Blends and Ionomers*; Utracki, L. A., Weiss, R. A., Eds.; ACS Symp. Ser. 395; American Chemical Society: Washington, DC, 1989; p 353.
(7) MacKnight, W. J.; Lenz, R. W.; Musto, P. V.; Somani, R. J. *Polym. Eng. Sci.* **1985**, *235*, 1124.
(8) Fairly, G.; Prud'homme, R. E. *Polym. Eng. Sci.* **1987**, *27*, 1495.
(9) Meyer, R. V.; Tacke, P. U.S. Patent 4,246,371, 1981.
(10) Lancaster, G. M.; Hoening, S. M. U.S. Patent 4,532,100, 1985.
(11) Matzner, M.; Schober, D. L.; Johnson, R. N.; Roberson, L. M.; McGrath, J. E. In Permeability of Plastic Films and Coatings; Hofenberg, H. B., Ed.; Plenum: New York, 1975; p 125.
(12) Kuphal, J. A.; Sperling, L. H.; Robeson, L. M. *J. Appl. Polym. Sci.* **1991**, *42*, 1525.
(13) Sullivan, M. J.; Weiss, R. A. *SPE ANTEC Tech. Pap.* **1991**, *37*, 964.
(14) Lu, X.; Weiss, R. A. *Polym. Mater. Sci. Eng.* **1991**, *64*, 163. Lu, X.; Weiss, R. A. *Macromolecules* **1991**, *24*, 4381.
(15) Lu, X.; Weiss, R. A. In *Symposium Proceedings of the Fall Meeting of the MRS*; Roe, R. J.; O'Reiilly, J. M., Eds.; Materials Research Society: Pittsburgh, 1991; p 29.
(16) Molnar, A.; Eisenberg, A. *Polym. Commun.* **1991**, *32*, 1001.
(17) Makowski, H. S.; Lundberg, R. D.; Singhal, G. H. U.S. Patent 3,870,841, 1975.
(18) Porod, G. *Kolloid Z.* **1951**, *124*, 83; **1952**, *125*, 51, 108.
(19) Hoffman, J. D.; Weeks, J. J. *J. Res. Natl. Bur. Stand.* **1962**, *66A*, 13.
(20) Nishi, T.; Wang, T. T. *Macromolecules* **1975**, *8*, 909.
(21) Fernandes, A. C.; Barlow, J. W.; Paul, D. R. *J. Appl. Polym. Sci.* **1984**, *29*, 1971.
(22) Lu, X.; Weiss, R. A. *Polym. Mater. Sci. Eng.* **1991**, *64*; *Macromolecules*, **1992**, *25*, 3242.
(23) Zundel, G. *Hydration and Intermolecular Interaction*; Academic Press: New York, 1969.
(24) Fitzgerald, J. J.; Weiss, R. A. In *Coulombic Interactions in Macromolecular Systems*; Eisenberg, A., Bailey, F. E., Eds.; ACS Symp. Ser. 302; American Chemical Society: Washington, DC, 1989; p 35.
(25) Fujimura, M.; Hashimoto, T.; Kawai, H. *Macromolecules* **1981**, *14*, 1309.
(26) Yarusso, D. J.; Cooper, S. L. *Macromolecules* **1983**, *16*, 1871.
(27) Fitzgerald, J. J.; Weiss, R. A. *J. Polym. Sci., Polym. Phys. Ed.* **1990**, *28*, 1719.
(28) Register, R. A.; Cooper, S. L. *Macromolecules* **1990**, *23*, 310.
(29) Ding, Y. S.; Hubbard, S. R.; Hodgson, K. O.; Register, R. A.; Cooper, S. L. *Macromolecules* **1988**, *21*, 1698.
(30) Galambos, A. F.; Stockton, W. B.; Koberstein, J. T.; Sen, A.; Weiss, R. A.; Russel, T. P. *Macromolecules* **1987**, *20*, 3091.